Chapter 3. Radial Waveguide for Solar Thermal Desalination

3.1. Introduction

The analytical closed form solution, the simulation method for the ray trace analysis, description of the loss mechanisms associated with the waveguides and a cost model for the radial waveguide are described in this chapter. Later in the chapter, a parametric study based on the ray trace simulation and a parametric study based on the analytical model has been presented. This is followed by a cost analysis and the optimal radial waveguide-receiver configuration that minimizes LCOP. The key findings and conclusions have been stated towards the end.

3.2 Analytical model for the radial waveguide

The design of a waveguide collector and its integration to the receiver is critical for CST applications. Figure 12 shows the schematic of a radial waveguide integrated to a linear receiver, also called a heat collection element, such as that commonly employed in parabolic trough CST power plants. The heat collection element (HCE) consists of an absorber pipe carrying heat transfer fluid (HTF) surrounded by an evacuated glass tube envelope. The waveguide radius and thickness are denoted by R_{wg}, t respectively; while the radius of the heat collection element is denoted by R_{rec}.

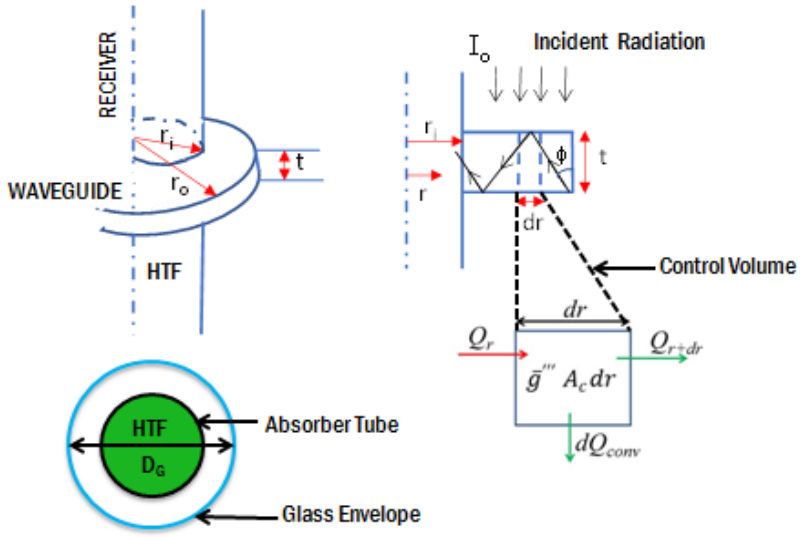

Figure 12. Schematic illustration of the radial waveguide concentrator integrated to a central receiver, and control volume showing the influx and out fluxes of heat

The waveguide is assumed to be made of the same material as that of the glass envelope of the receiver so that they have similar thermal coefficient of expansion for a perfect hermetic sealing. In an actual waveguide based solar concentration system, an array of cylindrical lenses forms the top layer that focuses the incident solar rays on to a coupling structure etched on the bottom layer of the waveguide. The rays reflected by the coupler at angles exceeding the critical angle would be totally internally reflected and transmitted to the two edges of the waveguide into the HCEs.

An analytical model is developed for the theoretically ideal waveguide concentrator depicted in Fig. 12. The goal is to develop an analysis that would present the theoretical maximum realizable performance of a waveguide based concentrator, which would form a target to achieve in practical desalination applications. The analysis assumes the following:

(a) Perfect focusing of the solar irradiation by the lenses on to the coupling structure, i.e. no focal dispersion of the rays at the focal point resulting in zero losses due to rays missing the coupler or coupled at an undesirable angle.
(b) Perfect total internal reflection with no escape cone losses.
(c) No waveguide decoupling loss due to the likelihood of the propagating rays striking a subsequent coupling feature during TIR.
(d) Stable and constant optical properties of the waveguide material over operating temperature range.
(e) Monochromatic incident light (optical properties invariant of wavelength).

For a perfectly transparent material exhibiting lossless TIR, all the incident irradiation should reach the two receivers coupled to the edges of the waveguide. Nevertheless, even transparent materials absorb some of the irradiation due to the extinction coefficient of the material that will attenuate the irradiation flux propagated to the ends. Considering that ray propagation is along r-direction only, with the incident light assumed to scatter uniformly over $0 \leq \phi \leq \frac{\pi}{2}$ (Fig. 12), the irradiation though an angle $d\phi$ is $I_0\,(2\pi r.\,dr).\frac{d\phi}{\pi/2}$. The attenuated intensity of solar irradiation reaching the receiver due to absorption coefficient (α) of the waveguide material is dependent on the path length of the solar rays traversing through the waveguide. The path length (λ) of light

entering at r through dr is $\lambda = \frac{r-R_{rec}}{Sin\ \phi}$. The total irradiation, I_t reaching a receiver through an edge can then be expressed as:

$$I_t(2\pi r_i.t) = \frac{I_0}{2\pi R_{rec}t}\int_{\phi=0}^{\phi=\frac{\pi}{2}}\int_{r=R_{rec}}^{r=R_{wg}} .e^{-\propto(r-R_{rec})/Sin\ \phi}.dr.d\phi \quad (3a)$$

which, when integrated over the outer receiver radius (R_{rec}) and outer waveguide radius (R_{wg}) results in the following expression:

$$I_t = \frac{2I_0}{\pi R_{rec}t}\int_0^{\frac{\pi}{2}}\left(\frac{\sin\phi}{\alpha}\right)^2\left(1-e^{-R^*}\right)-\left(\frac{\sin\phi}{\alpha}\right)\left(R_{wg}e^{-R^*}-R_{rec}\right).d\phi \quad (3b)$$

where $R^* = \frac{\alpha(R_{wg}-R_{rec})}{sin\ \phi}$. Assuming all the incident irradiation energy are transferred as heat to the heat transfer fluid (HTF) in the HCE at a thermal efficiency of η_R, the thermal power (P_t) delivered to the linear receiver per unit waveguide based on a simple energy balance follows:

$$P_t = \dot{m}_F c_F(T_{F,out}-T_{F,in}) = N_{wg}\times I_t(2\pi R_{rec}t)\cdot\eta_R \quad (4)$$

where N_{wg} is the number of waveguides, $\dot{m}_F$ is the mass flow rate of the HTF, C_F is the specific heat of the HTF, $T_{F,in}$ is the HTF inlet temperature and $T_{F,out}$ is the HTF outlet temperature. The thermal efficiency of the receiver (η_R) is given by:

$$\eta_R = \beta\tau - \frac{h(2R_{rec}+2t)\times(T_{Red}-T_{amb})}{I_t\times t} \quad (5)$$

where β and τ are the absorptivity and transmissivity of the receiver glass envelope, respectively; h is the convective heat transfer coefficient, T_{Rec} is the receiver glass envelope temperature, and T_{amb} is the ambient temperature.

The governing equation for steady state temperature distribution along the radius of the waveguide concentrator can be obtained from the conservation of energy principle applied to the differential control volume, *dr*, in Fig. 12. Referring to Fig. 12, $-k\frac{dT}{dr}$ is the heat transfer rate due to thermal conduction, k is the thermal conductivity of the material, and h is the convective heat transfer coefficient due to thermal interaction with ambient air. The appropriate form of the energy conservation equation is as follows:

$$\frac{d^2T}{dr^2} + \frac{1}{r} \cdot \frac{dT}{dr} - \frac{2h}{kt}\,(T - T_{amb}) + \frac{\bar{g}'''}{k} = 0 \tag{6}$$

where $\bar{g}'''$ is the volumetric generation due to the irradiation absorption within the waveguide, which is assumed to be uniformly distributed within the volume of the waveguide:

$$\bar{g}''' = \frac{I_0\pi(R_{wg}^2 - R_{rec}^2) - I_t(2\pi R_{rec}t)}{\pi(R_{wg}^2 - R_{rec}^2)t} \tag{7}$$

Solution to Eq. (6) can be obtained as a combination of general solution and particular solution leading to the following expression:

$$\theta(r) = C_1 I_0(r^*) + C_2 K_0(r^*) + \frac{\bar{g}'''}{m^2 k} \tag{8}$$

where $r^* = mr$, $m = \sqrt{\frac{2h}{kt}}$, $\theta = T - T_{amb}$. I_0 and K_0 are zeroth order modified Bessel function of the first and second kind, respectively. C_1 and C_2 are the coefficients to be determined from appropriate boundary conditions. Since the waveguide concentrator is bonded to the glass envelope of the receiver, the temperature at the inner radius of the waveguide concentrator is the receiver glass envelope temperature as identified by Eq. (9a). The outer edge of the waveguide is an active convective tip. Nevertheless, since, $R_{rec} \gg t$, an adiabatic boundary condition is assumed and a corrected outer radius of $R_{rec} + {}^{t}/_{2}$ is substituted in the resulting final expression to capture the effect of convective loss at the outer edge on the temperature distribution within the waveguide [63]. The boundary conditions can be mathematically expressed as:

$$\theta(r = R_{rec}) = \theta_{Rec} \tag{9a}$$

$$\frac{d\theta}{dr}\left(r = R_{wg}\right) = 0 \tag{9b}$$

The evaluation of coefficients C_1 and C_2 require only two boundary conditions. Eqs. (9a) and (9b) are utilized to determine the coefficients. The acquired expression for the steady state temperature distributio8n along the radial of the planar waveguide concentrator in dimensionless form is:

$$\frac{\theta(r)}{\theta_{Rec}} = R_g + \left[1 - R_g\right]\left\{\frac{K_1(r_0{}^*).I_0(r^*) + I_1(r_0{}^*).K_0(r^*)}{K_1(r_0{}^*).I_0(r_i{}^*) + I_1(r_0{}^*).K_0(r_i{}^*)}\right\} \tag{10}$$

I_1 and K_1 are first order modified Bessel function of the first and second kind, respectively; and $R_g = \frac{\bar{g}'''}{m^2 k \theta_{Rec}}$ where $\theta_{Rec} = T_{Rec} - T_{amb}$. A quick verification by substituting $\bar{g}''' = R_g = 0$ in the acquired solution, Eq. (10) verifies the validity of the solution as it reduces to the expression for temperature distribution in a radial fin as reported in Incropera et al. [63]

3.3 Simulation and parametric study for the radial waveguide

The thermal and optical analysis of the waveguide was conducted using TracePro. The lens array and waveguide were designed in CAD software with the required specification and then imported into TracePro for the analysis. The lens array and waveguide were assigned properties of Schott BK7 and Schott F2 glass respectively. The lens array and the waveguide were assembled as shown in Figure 13a. The rays would pass through the lens array and converge towards the scattering surface and then undergo total internal reflection as shown in figure 13b. The grating surface is made as shown in figure 13c and it consists of 6 reflecting surfaces. The angle included between the reflecting surface is kept constant at 120^0. The source for the radiation is placed above the lens surface and the intensity and wavelength of the radiation is varied for the different studies. The rays have been traced for the various combinations of parameters and the collection efficiency at the center of the radial waveguide along with the total energy collected is recorded. The energy incident on the lens surface is kept constant at 1000 W/m^2. The decoupling loss which occurs when a ray undergoing total internal reflection is incident on the scattering surface and then escapes the waveguide is also recorded. The energy lost due to absorption while travelling through the waveguide material is also recorded.

3.4 Loss mechanisms associated with waveguides

The energy collected at the center of the radial waveguide is only a part of the energy incident on the lens surface. There are losses associated with every step from the light striking the lens surface to the point when the light strikes the energy absorbing surface. The Figure 14 shows the various loss mechanisms involved in energy collection through waveguides.

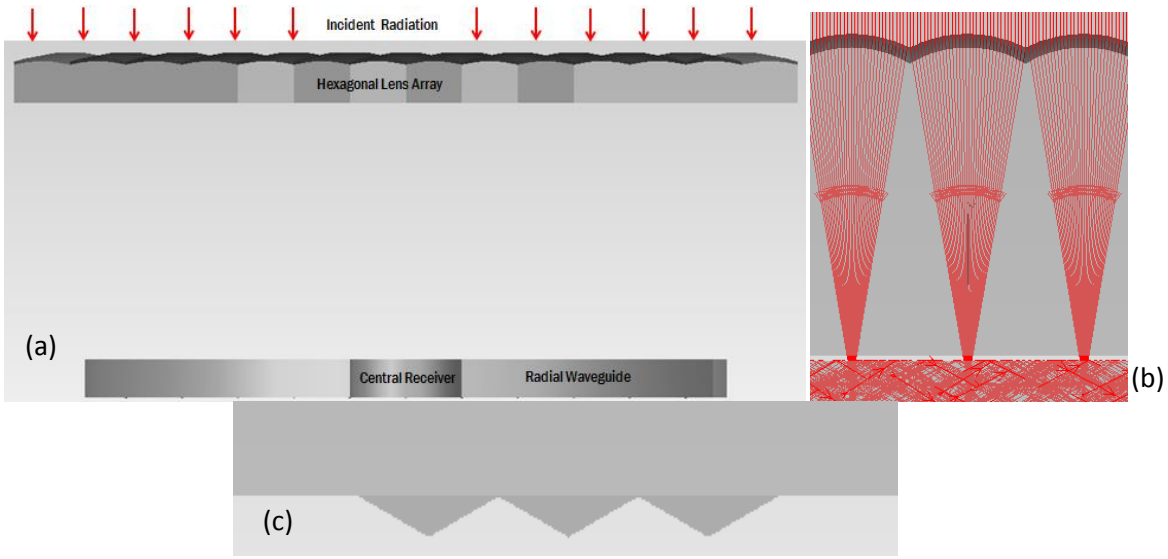

Figure 13. (a) Simulation setup for the radial waveguide (b) rays undergoing total internal reflection in the waveguide (c) cross section of the scattering surface

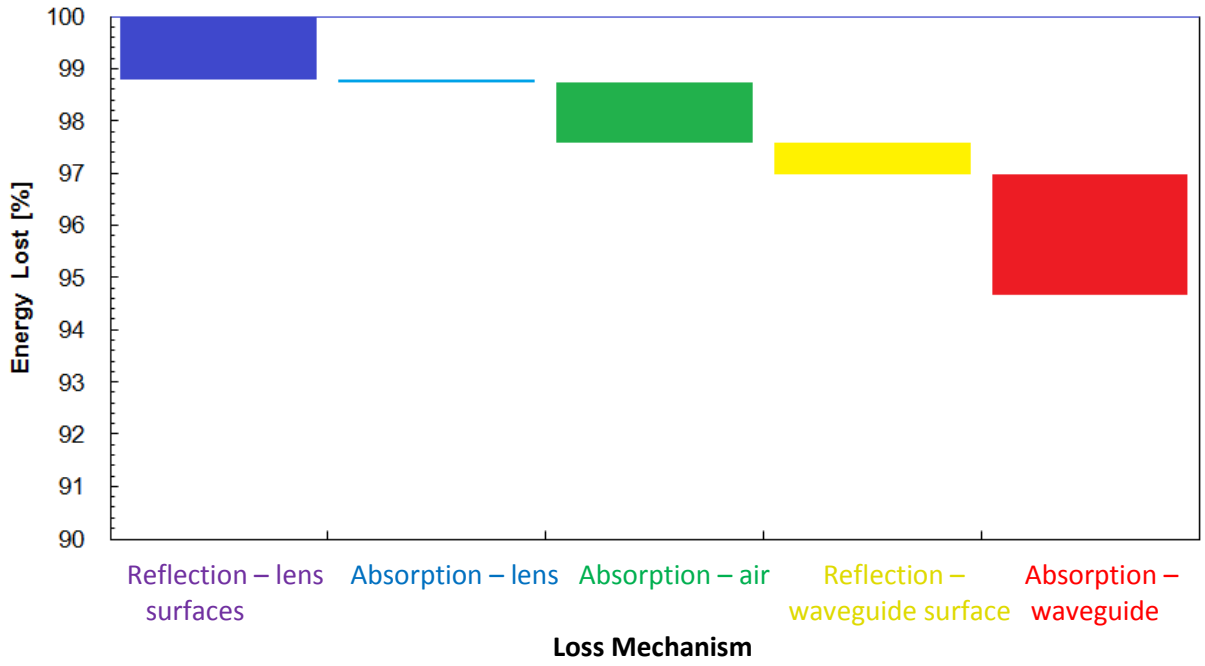

Figure 14. Waterfall chart showing the various loss mechanisms for solar energy concentration through a waveguide.

The first stage of energy loss is when the rays strike the lens surface. At this point, some of the energy is reflected back into the atmosphere. The extent of this loss can be limited by using antireflective coatings like MgF_2. A single layer of antireflective MgF_2 coating is used in this

case and it has limited the loss at this stage to 0.6% for each of the lens surfaces and since there are two lens surfaces, top and bottom, the total loss due to reflection at the lens surface is about 1.2%. There is a small amount of energy lost due to absorption in the lens material. This loss is usually insignificant as the rays travel for a very small distance through the lens which is roughly equal to the thickness of the lens array. The air gap between the lens surface and the waveguide, which is essential to make sure that the scattering surface coincides with the lens focus, leads to some loss due to absorption of the radiation in air. A considerable amount of energy losses occur due to absorption through the waveguide material. This loss will depend on the size of the waveguide which directly affects the distance the rays travel before they are absorbed by the energy absorbing surface at the center of the waveguide. The loss due to reflection at the top surface of the waveguide is limited by using the antireflective MgF_2 coating. There are two more loss mechanisms in which the rays escape the waveguide. First is the loss which occurs when the rays passing through the lens array are not focused on the scattering surface properly and directly pass through the waveguide. This loss is prominent when the either the waveguide is not aligned properly with the lens array or the scattering surface is small and all rays passing through the lenses cannot be focused on the scattering surface. The second prominent loss in which the rays escape the waveguide is the decoupling loss. It occurs when a ray undergoing total internal reflection and travelling through the waveguide strikes the scattering surface and then decouples as the angle of incidence becomes less than the critical angle and it passes through the waveguide surface and escapes. This loss increases as the size of the waveguide increases as the rays travel longer to reach the absorbing surface and because of this the probability of it undergoing decoupling increases. The size of the scattering surface has an effect on this loss. The probability of a ray undergoing decoupling increases as the size of the scattering surface increases and this leads to greater losses. Therefore, the size of the scattering surface has to be optimized as it has a great effect on the overall collection efficiency of the waveguide.

3.5 Cost model for the radial waveguide

The present work also incorporates a simple cost model to evaluate the optimal design configurations based on minimizing cost. The total cost of the system (C_t) comprises of both receiver and waveguide subsystems, which can be expressed in the form of cost per unit aperture area (C'') as:

$$C'' = \frac{C_t}{N_{wg} * \pi(R_o^2 - R_i^2)} = \underbrace{\frac{C_R^{'} * (2t + 2R_o)}{\pi(R_o^2 - R_i^2)}}_{C_R^{''}} + \underbrace{\bar{C}_G \rho_G \cdot t}_{C_{W_G}^{''}} \quad (11)$$

where $C_R^{'}$ is the cost per unit width of the receiver (\$/m), $\bar{C}_G$ is the cost per unit mass of the waveguide material (\$/kg), $C_R^{''}$ is the receiver cost per unit aperture area (\$/m^2), $C_{W_G}^{''}$ is the waveguide cost per unit aperture area (\$/m^2) and ρ_G is the density of the waveguide material. In addition to the cost per unit area, a levelized cost of power (LCOP) is also evaluated to identify configurations that yield cost reductions, while simultaneously maximizing the net thermal power delivered to the receiver. The levelized cost of power (LCOP) in \$/W is expressed as:

$$\text{LCOP} = \frac{C''}{\eta_C * I_o} = \frac{C_R^{'} * (2t + 2R_o)}{P_t} + \frac{\bar{C}_G * (\rho_G * t) * \pi(R_o^2 - R_i^2)}{P_t} \quad (12)$$

where η_C is the collection efficiency defined as $\eta_C = \frac{P_t}{I_o * \pi(R_o^2 - R_i^2)}$, I_o is the incident solar irradiance and P_t is the net power delivered to the receiver. The cost per unit length of the receiver ($C_R^{'}$) is taken as 150 \$/m based on state-of-art Ultimate Trough evacuated tube receiver concept [64], the density of the waveguide material (ZK7) is tabulated in Table 1 and the cost of glass is taken to be 2.25 \$/kg [65]. It is to be noted that the cost of support structures and pylons, drive systems, electronics and control, foundations, etc., which are a major part of parabolic trough collector cost [66] are negligible for waveguide-receiver system due to its compact, lightweight nature and possible non-tracking implementation. Hence, although the cost model introduced here is intended to be simple, it is a fairly accurate representation of large-scale planar waveguide concentrator-receiver system.

Table 2. Thermophysical properties of optical glass (ZK7) used in this study

Properties	Values
Density, ρ [kg/m^3]	2490.0
Thermal conductivity, k [W/m-K]	1.1
Thermal stress factor, φ [MPa/K]	0.4
Absorption coefficient, α [m^{-1}]	1.4
Transformation temperature, T_g [°C]	539.0

3.6 Analysis Methodology

The present study evaluates the influence of the two design or material parameters—waveguide thickness (t) and radius (R_{wg})—and the operating parameter namely, the incident irradiation (I_0) on the steady-state dimensionless temperature distribution (θ) and net thermal power delivered (P_t). The radius (R_{wg}) and thickness (t) of optical glass waveguide, such as BK7 or ZK7, is varied between 0.1 m to 2 m, 3 mm to 50 mm, respectively, while the solar spectral averaged absorption coefficient is ~1.4 m^{-1} [67,68]. Table 1 provides the thermo-physical properties of ZK7 glass obtained from literature [67-69]. The incident solar irradiation (I_0) is varied between 500 W/m^2 to 1000 W/m^2 to investigate radial waveguide designs for various geographical locations.

It is reasoned that the waveguide design will be limited by the maximum temperature within the waveguide material that occurs when the convective heat transfer between the waveguide and ambient is at its lowest. Accordingly, the convective heat transfer coefficient, h, is chosen to be that of buoyancy-induced convection from a heated, horizontal rectangular surface to a quiescent ambient [63], which evaluates to ~2.5 to 5.0 W/m^2-K. The receiver glass radius (R_{wg}) is assumed to be 40 mm, similar to that of commercially available Schott's parabolic trough receivers [71,72]. As a result, the parametric range of receiver glass temperature is determined from the literature [71,72] that characterizes the trend and magnitude of receiver glass temperature as a function of heat transfer fluid temperature (T_F) within the absorber tubes. Since the receiver glass envelope is essentially opaque to infra-red energy, all the thermal losses from the receiver must pass, via conduction, through the glass envelope. As a result, the radiant and convective thermal losses from the receiver are directly related to the glass envelope temperature (T_{Rec}), regardless of what happens inside the absorber tube.

Based on the data obtained from Price et al. [71] for air speed of 0 m/s and ambient temperature of 35 ℃ the correlation for the receiver glass envelope temperature (T_{Rec} in ℃) as a function of HTF temperature (T_F in ℃) inside the absorber tubes can be expressed as:

$$T_{Rec}[℃] = 51.96 \times 10^{-5} \cdot T_F^2 - 89.63 \times 10^{-3} \cdot T_F + 53.36 \qquad (13)$$

For desalination applications, the required HTF temperature is ~ 100 ℃ [53], corresponding to which the receiver temperature based on the correlation is 50 ℃. With increase in wind speed,

the glass envelope temperature will decrease due to forced convection cooling and Ref. [71] also provides the characteristic curves for various wind speeds. However, based on the same rationale discussed above for the choice of minimum convective heat transfer coefficient value, the design of the waveguide concentrator will be limited by the maximum material temperature corresponding to quiescent (zero wind speed) conditions, which is of interest in this study.

3.7. Results and Discussion

3.7.1 Parametric Analysis based on Simulations

3.7.1.1 Effect of Grating size

The grating size affects the overall collection efficiency and hence the energy collected at the collection surface. Decoupling losses and the losses due to the rays passing through the waveguide are greatly affected by the grating size. The grating is square in shape and its cross section is as shown in Figure 13c. It consists of six reflecting surfaces and all of them have an included angle of 120^0. For this study, the side of the square scattering surface is varied from 60 µm to 150 µm. The other parameters for the waveguide and lens array were kept constant. The waveguide radius was 60 mm and the receiver radius was 30 mm. The thickness of the waveguide was 5mm, the focal length of the lens array was 19.09 mm and the pitch of the lens in the hexagonal lens array was kept constant at 4.5 mm. The graph in Figure 15a shows the variation of collection efficiency with grating dimension. It can be seen that the collection efficiency and the energy collected increases sharply from 60 µm to 78 µm. This is because of the fact that a huge percentage of rays pass through the waveguide without getting totally internally reflected at 60 µm. It can be seen in Figure 15b that there is a sharp decrease in the number of rays that pass through the waveguide when the grating size is increased from 60 µm to 78 µm. From 78 to 150 µm, the percentage of rays passing through the waveguide decreases at a lesser rate. It can also be seen from the same graph that the decoupling losses steadily increase as the grating size is increased from 60 to 150 µm. In the Figure 15c which shows the variation of the collection efficiency as the scattering dimension varies from 78 to 150 µm shows that the highest collection efficiency is achieved when the scattering dimension is 120 µm. For values higher than 120 µm, the value of the collection efficiency starts decreasing due to higher decoupling losses. The variation of absorption and decoupling loss is shown in Figure 15d. The

absorption loss is somewhat constant which is expected in this case since there is no variation in the dimensions of the waveguide which is the major parameter on which the absorption loss depends. The decoupling loss on the other hand increases steadily as the scattering dimension increases.

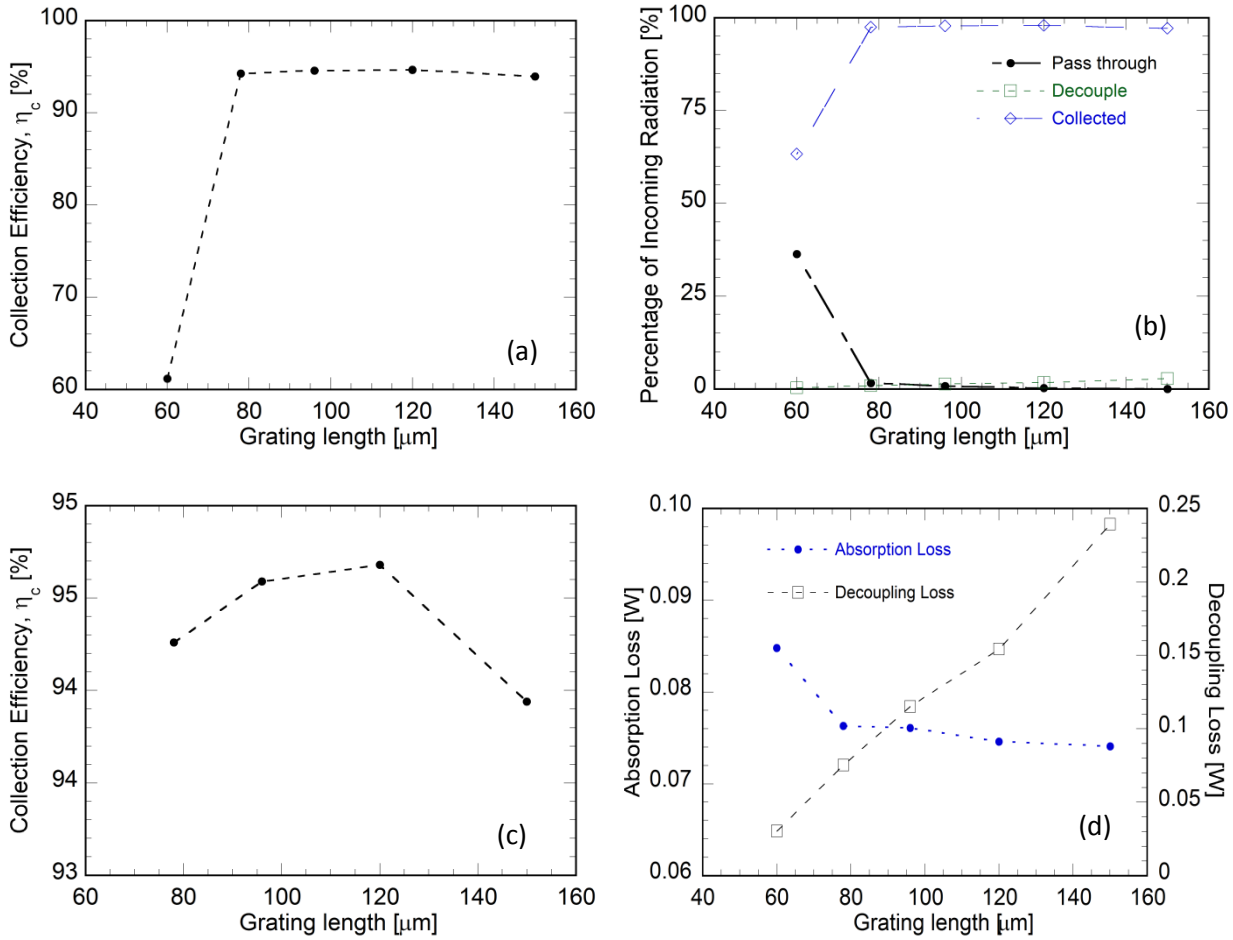

Figure 15. Effects of grating dimension on the (a) collection efficiency for the range 60 to 150 μm (b) percentage of rays collected (c) collection efficiency for the range 78 to 150 μm (d) absorption and decoupling losses

3.7.1.2 Effect of Waveguide Radius

For this study, the waveguide radius was varied from 100 mm to 500 mm. The other parameters for the waveguide and lens array were kept constant. The scattering surface dimension was 120 μm. The thickness of the waveguide was 5mm, the focal length of the lens array was 19.09 mm and the pitch of the lens in the hexagonal lens array was kept constant at 4.5 mm. The waveguide radius affects the collection efficiency and the energy collected in different

ways. The energy collected as can be seen from the graph in Figure 16 increases as the waveguide radius increases. This is due to the fact that the total energy incident on the waveguide surface increases as the area of the waveguide exposed to the sun increases. The collection efficiency decreases as the size of the waveguide increases because the rays have to travel for a longer distance to reach the collection surface and this leads to greater absorption and decoupling losses which can be seen from the graph in Figure 16.

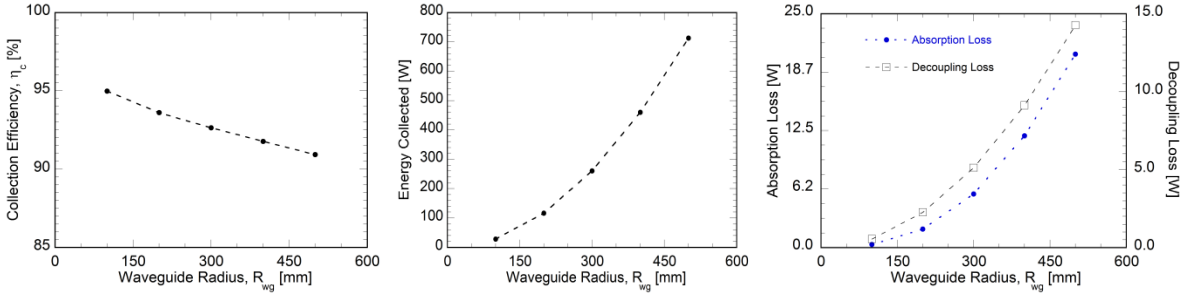

Figure 16. Effects of waveguide radius on the collection efficiency, energy collected and absorption and decoupling losses

3.7.1.3 Effect of Receiver Radius

The receiver radius has a substantial effect on the efficiency and the energy collected by the waveguide. All parameter other than the receiver radius were kept constant. The pitch of the hexagonal lens array was kept constant at 2.38 mm, the waveguide thickness at 5 mm, waveguide radius at 570 mm, the scattering surface dimension at 120 µm and the focal length at 16.83 mm. The receiver radius was varied from 10 mm to 50 mm. The effect on the collection efficiency and the collected energy can be seen in the graph in Figures 17. Both plots follow a similar trend. They increase, first reach a maximum value and then decrease. This is due to competing forces. The absorption and decoupling losses decrease when the receiver radius is increased as the distance which the rays have to travel decreases. At the same time an increase in the receiver radius leads to a part of radiation being lost as they are incident on the part of the waveguide which is hollow.

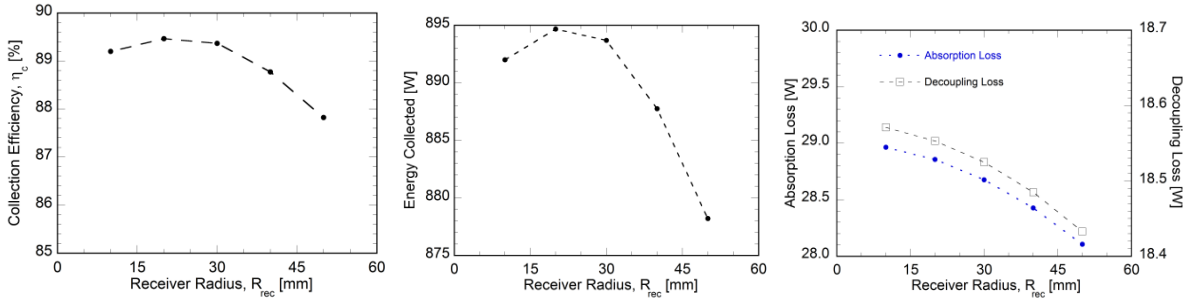

Figure 17. Effects of receiver radius on the collection efficiency, energy collected and absorption and decoupling losses

3.7.1.4 Effect of Waveguide Thickness

The absorption loss leads to generation of heat in the waveguide and that in turn leads to temperature rise in the waveguide. The temperature of the waveguide cannot be allowed to rise unchecked as the material which is being used as the waveguide, BK7 in this case has a specified temperature range in which it can be used. Increasing the thickness of the waveguide distributes the heat generated in the waveguide to a greater volume and so, the rise in temperature is less. The effect of varying the waveguide thickness in the range on 1 to 5 mm is not very significant on the collection efficiency or the losses as can be seen from the plots in Figure 18. Thus the only reason for increasing the waveguide thickness is to keep the temperature in check and within the working limits of the material.

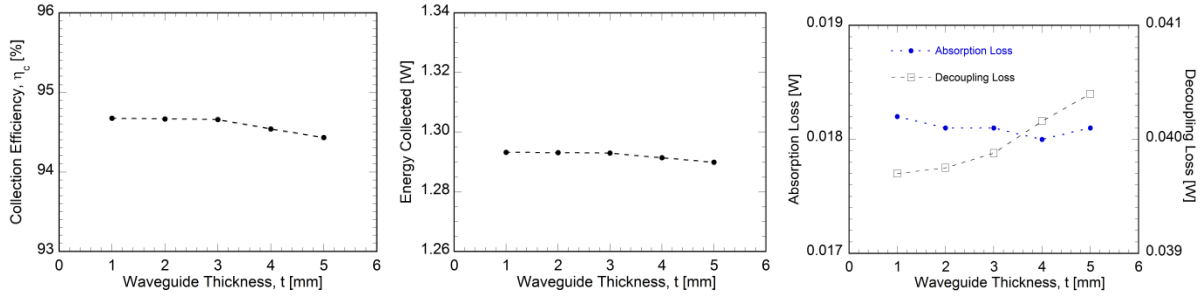

Figure 18. Effects of waveguide thickness on the collection efficiency, energy collected and absorption and decoupling losses

3.7.2 Parametric Analysis based on Analytical Model

The analytical model is first verified against the results from the ray trace simulations and the results have been plotted in Figure 19. The values of collection efficiency, energy collected and